The Journal of Veterinary Medical Science

NOTE

Pathology

Ultrastructural features of canine neuroaxonal dystrophy in a Papillon dog

Miyuu TANAKA[1)], Shinobu YAMAGUCHI[3)], Hideo AKIYOSHI[2)], Masaya TSUBOI[4)], Kazuyuki UCHIDA[4)], Takeshi IZAWA[1)], Jyoji YAMATE[1)] and Mitsuru KUWAMURA[1)]*

[1)]Laboratory of Veterinary Pathology, Graduate School of Life and Environmental Science, Osaka Prefecture University, Rinkuu Ourai Kita 1-58, Izumisano, Osaka 598-8531, Japan
[2)]Laboratory of Veterinary Surgery, Graduate School of Life and Environmental Science, Osaka Prefecture University, Rinkuu Ourai Kita 1-58, Izumisano, Osaka 598-8531, Japan
[3)]Hataeda Animal Hospital, 680 Iwakura Hataedacho, Sakyo-ku, Kyoto 606-0015, Japan
[4)]Laboratory of Veterinary Pathology, Graduate School of Agricultural and Life Sciences, The University of Tokyo, 1-1-1 Yayoi, Bunkyo, Tokyo 113-8657, Japan

J. Vet. Med. Sci.
79(12): 1927–1930, 2017
doi: 10.1292/jvms.17-0487

Received: 29 August 2017
Accepted: 2 October 2017
Published online in J-STAGE: 10 October 2017

ABSTRACT. Neuroaxonal dystrophy (NAD) is a neurodegenerative disease characterized by severe axonal swelling (spheroids) throughout the nervous system. In dogs, NAD has been reported in several breeds and a missense mutation in *PLA2G6* gene has recently been identified in the Papillon dog NAD. Here we performed ultrastructural analysis to clarify the detailed ultrastructural features of the Papillon dog NAD. Dystrophic axons consisted of accumulation of filamentous materials, tubulovesicular structures, and swollen edematous mitochondria with degenerated inner membranes were often observed in the central nervous system. At axonal terminals, degeneration of presynaptic membrane was also detected. As reported in *Pla2g6* knockout mice, mitochondrial and presynaptic degeneration may be related with the pathogenesis of NAD in Papillon dogs.

KEY WORDS: electron microscopy, mitochondria, neuroaxonal dystrophy, papillon, PLA2G6

Canine neuroaxonal dystrophy (NAD), an inherited neurodegenerative disease characterized by severe axonal swelling (spheroids) throughout the nervous system, has been reported in several breeds including Papillons, Rottweilers, Chihuahuas, Collie sheepdogs, Jack Russell Terriers, Spanish water dogs, crossbreed laboratory dogs and Dachshund-cross dogs [2, 4–6, 9, 13–15, 18, 21]. Recently, a missense mutation in *PLA2G6* gene, encoding a calcium-independent group VI phospholipase A2 beta (iPLA2β), has been identified in the Papillon dog NAD [20]. A number of *PLA2G6* mutations have also been identified in 80–85% of human patients with infantile neuroaxonal dystrophy (INAD), also known as neurodegeneration with brain iron accumulation (NBIA) 2A, characterized by early onset and rapid progression of various neurological symptoms [7, 8, 12, 16]. Mutations in *PLA2G6* gene have variable phenotypic outcomes, so these different clinical groups have recently been collectively referred to as *PLA2G6*-associated neurodegeneration (PLAN) [10]. The detailed mechanism of INAD, and the relationship between *PLA2G6* dysfunction and neuroaxonal degeneration remain unclear. *Pla2g6* knockout (KO) mice and *Pla2g6*-mutated mice have been established [1, 11, 17, 19, 22, 23], and ultrastructural analysis of *Pla2g6* KO mice indicated that degeneration of mitochondrial inner membranes and presynaptic membranes appear to underlie INAD pathology [1, 19]. In the Papillon dog NAD, immunohistochemical features of spheroids have been well investigated; many spheroids showed strong immunoreactivity for neurofilaments (NFs), synaptophysin and a large number of calcium-binding protein-positive spheroids were detected in the cerebellum, medulla oblongata [13, 20]. However, detailed ultrastructural features of the Papillon dog NAD have not yet been investigated. In the present study, we performed ultrastructural analysis on the central nervous system (CNS) to clarify the detailed ultrastructural features of the dystrophic axons in a Papillon dog with NAD.

A male Papillon pup could not walk until 2 months of age and was suspected to be blind. Neurological symptoms including intension tremor, limb extension and astasia were observed at 3 months of age. At 4 months of age, this dog was referred to the Veterinary Medical Center of Osaka Prefecture University and MRI examination revealed only mild cerebellar atrophy. Because of poor prognosis, the dog was euthanized by the owner's request. At necropsy, there was no significant gross findings in the CNS other than mild cerebellar atrophy. Tissue samples from the CNS were fixed in 10% neutral-buffered formalin, embedded in paraffin. Sections of 4 μm thick were cut and stained with hematoxylin and eosin (HE). Formalin-fixed tissues were also stored in

*Correspondence to: Kuwamura, M.: kuwamura@vet.osakafu-u.ac.jp

2.5% glutaraldehyde in 0.1 M phosphate buffer (PB; pH 7.4), post-fixed with 1% osmic tetraoxide at 4°C overnight, and embedded in epoxy resin. One-μm semi-thin sections were cut and stained with toluidine blue (TB) for light microscopy. Ultrathin sections were stained with uranyl acetate and lead citrate and examined in a Hitachi H-7500 electron microscope (Hitachi, Tokyo, Japan).

Histopathologically, dystrophic swollen axons were found throughout the CNS, and the spheroids showed varied sizes and heterogeneous morphology; homogeneous and granular appearance with or without clefts and vacuoles (Figs. 1 and 2). Some spheroids had a densely stained or granular central core structure in TB stained semi-thin sections (Fig. 2). A number of axonal spheroids were predominantly localized in the dorsal horn of spinal cord, cerebellum and medulla oblongata including nuclei cuneatus, nuclei gracilis, nuclei olivalis, nuclei spinalis nervi trigemini and lemniscus medialis. These spheroids showed strong immunoreactivity for synaptophysin and NFs markers (data not shown) similar to previous reports [13]. From these histological features, this case was diagnosed as NAD. As previously reported by Tsuboi *et al*., a missense mutation in the patatin domain of *PLA2G6* gene (c.1579G>A) was identified in this dog by whole exome sequencing analysis and TaqMan genotyping assays [20].

Transmission electron microscopic observation revealed that axonal spheroids consisted of accumulation of filamentous and granular materials, tubulovesicular structures (Figs. 3a, 3b and 3e: white asteristks) and densely packed mitochondria, as well as edematous vacuoles, vesicular structures and electron-dense bodies (Fig. 3a–d) in the CNS. It is noteworthy that numerous swollen edematous mitochondria with degenerated inner membranes were often observed in the spheroids and axons (Fig. 3d–g: arrowheads); some abnormal mitochondria were also detected in presynapses (Fig. 3e and 3f). In these abnormal mitochondria, cristae were diffusely degenerated, branching and tubular appearance. Abnormally degenerated mitochondria were also detected in neurons (Fig. 3h: Purkinje cell, arrowheads). Some abnormal mitochondria were surrounded by membrane structures, suggesting mitophagy (Fig. 3h: inset). There were only a few mitochondria or mitochondria-like structures containing dense granules (data not shown). In addition, the presynaptic membranes were degenerated and expanded irregularly in axonal terminals (Figs. 3e and 3f).

Canine NAD has previously been reported in several breeds [2, 4–6, 9, 13–15, 18, 21], but both ultrastructural and genetic/molecular analyses have been performed for a few cases. For example, spheroids consisted of the accumulation of autophagosomes in Spanish water dogs with a tectonin beta-propeller repeat-containing protein 2 (*TECPR2*) mutation [9]. In laboratory dogs (crossbreed of Giant Schnauzer and Beagle) with a *mitofusin 2* (*MFN2*) mutation, dystrophic axon showed accumulations of membrane-bound vesicles containing variably electron-dense materials and organelles such as fragmented degenerating mitochondria (mitophagy) [5, 6]. In our case, there were no accumulated autophagosome, but we found some abnormal mitochondria or dense bodies surrounded by membrane structures. Immunohistochemical approach will be helpful to investigate involvement of autophagy or mitophagy in the pathogenesis of Papillon dog NAD with a *PLA2G6* mutation.

In this report, we performed detailed ultrastructural analysis on the CNS in a Papillon dog with NAD and revealed that ultrastructural features of axonal spheroid were closely similar to human INAD [3, 24] and INAD mouse models [1, 19, 22, 23]. In addition to the accumulation of tubulovesicular structures in spheroids (a pathological hallmark of INAD), it is noteworthy that densely packed mitochondria and numerous swollen edematous mitochondria with degenerated inner membranes were detected in the spheroids and axons. These result suggested that the Papillon dog NAD with a missense mutation in the *PLA2G6* gene seems to have similar mitochondrial pathology with human and mouse INAD.

In mice, two types of INAD models have been established: *Pla2g6*-KO (null mutation) mouse and *Pla2g6-inad* mouse with a point mutation in the ankyrin domain of *Pla2g6*. Both of INAD mouse models have no phospholipase enzymatic activity, but the clinical course and ultrastructural findings are different. In *Pla2g6*-KO mouse, the clinical onset was critically late and neurological abnormalities developed slowly [1, 17, 19]. On the other hand, *Pla2g6-inad* mouse showed early onset of clinical symptoms and progressed rapidly, and then all of the homozygous mice died before 18 weeks of age [22, 23]. Ultrastructurally, typical tubulovesicular structures were detected in both mouse models [1, 19, 23]. In *Pla2g6*-KO mouse, mitochondrial and presynaptic membrane abnormalities also developed from an early stage of disease (presymptomatic stage); mitochondrial inner membranes degenerated into granular materials, and mitochondria with tubulovesicular cristae were frequently observed in later stage of disease. This indicated that specific degeneration of inner mitochondrial and presynaptic membranes underlie INAD pathology [1, 19]. Most cases of Papillon dog NAD are considered to be an early onset [20], and the present case already had prominent mitochondrial abnormalities in the CNS, which correspond to those in later stage of *Pla2g6*-KO mouse. In our Papillon dog (intermediate to late clinical stage) and *Pla2g6-inad* mouse, no or only a few abnormal mitochondria containing dense granules considered to be degenerated inner membrane were observed. This may reflect the differences in the disease stage or rate of progression. It would be important to study the relationship between the ultrastructural features of neuronal/axonal abnormalities and the disease stage or severity. Furthermore, phenotypic differences among these INAD cases could be caused by the pattern of the existence of mutated PLA2G6 protein and variations of mutated positions.

In human INAD, axonal spheroids contain tubulovesicular or tubulomembranous structures, aggregation of mitochondria, vesicules and membranous bodies [3, 24]. Detailed mitochondrial changes, such as degenerating changes and branching tubular cristae, were also mentioned [1, 3]. These mitochondrial abnormalities were similar to our case and INAD mouse models, but further accumulation of ultrastructural analysis data about human INAD cases is needed for detailed comparative analysis with animal models.

Taken together, our detailed ultrastructural study revealed that degeneration of mitochondrial inner membrane and presynaptic membrane may be related with the pathogenesis of NAD in Papillon dogs, and NAD-affected Papillon dogs could be valuable animal model for human INAD. Establishment of new rodent model that bears a missense mutation in the same domain as Papillon dog NAD might be also a favorable tool for further studies. The comparative analyses of different mutated types of INAD animal models may clarify the pathogenesis of PLAN including INAD.

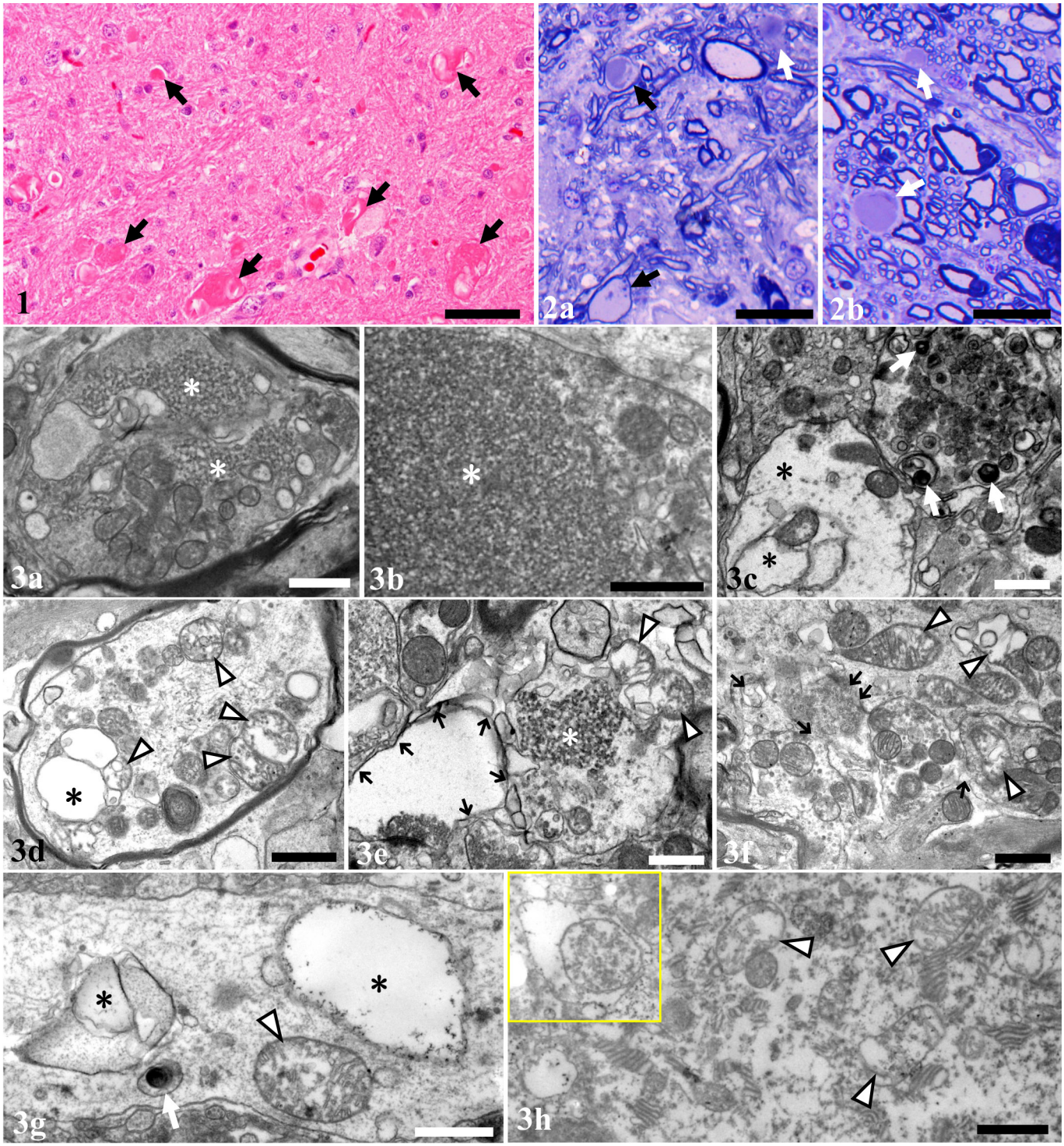

Fig. 1. The spheroids (arrows) vary in sizes from 10 to 50 μm and show various morphologies. Some spheroids contains clefts or vacuoles. Medulla oblongata. HE. Bar=50 μm.

Fig. 2. The spheroids show homogenous appearance or contain granular material and dense central core with thin myelin (black arrows) or without myelin (white arrows). Spinal cord, gray (a) and white (b) matter. TB, semi-thin section. Bar=25 μm.

Fig. 3. Axonal spheroids are filled with tubulovesicular structures (a, b and e: white asterisks), granular or filamentous materials (d), edematous vacuoles (c, d and g: black asterisks), dense bodies (c and g: white arrows) and densely packed mitochondria (a). Swollen mitochondria with degenerated inner membranes, characterized by degenerated branching and tubular cristae, are also observed (d–g: arrowheads). In the axonal terminals, presynaptic membranes expand irregularly, and membranous degeneration is observed (e and f: black arrows). Abnormal mitochondria, sometimes surrounded by membrane structures (h: inset), are also detected in the Purkinje cells (h: arrowheads). (a–f) spinal cord, (g) cerebrum, (h) cerebellum. Transmission electron microscopy. Bar=1 μm.

REFERENCES

1. Beck, G., Sugiura, Y., Shinzawa, K., Kato, S., Setou, M., Tsujimoto, Y., Sakoda, S. and Sumi-Akamaru, H. 2011. Neuroaxonal dystrophy in calcium-independent phospholipase A2β deficiency results from insufficient remodeling and degeneration of mitochondrial and presynaptic membranes. *J. Neurosci.* **31**: 11411–11420. [Medline] [CrossRef]
2. Degl'Innocenti, S., Asiag, N., Zeira, O., Falzone, C. and Cantile, C. 2017. Neuroaxonal Dystrophy and Cavitating Leukoencephalopathy of Chihuahua Dogs. *Vet. Pathol.* **54**: 832–837. [Medline] [CrossRef]
3. de León, G. A. and Mitchell, M. H. 1985. Histological and ultrastructural features of dystrophic isocortical axons in infantile neuroaxonal dystrophy (Seitelberger's disease). *Acta Neuropathol.* **66**: 89–97. [Medline] [CrossRef]
4. Diaz, J. V., Duque, C. and Geisel, R. 2007. Neuroaxonal dystrophy in dogs: case report in 2 litters of Papillon puppies. *J. Vet. Intern. Med.* **21**: 531–534. [Medline] [CrossRef]
5. Fyfe, J. C., Al-Tamimi, R. A., Liu, J., Schäffer, A. A., Agarwala, R. and Henthorn, P. S. 2011. A novel mitofusin 2 mutation causes canine fetal-onset neuroaxonal dystrophy. *Neurogenetics* **12**: 223–232. [Medline] [CrossRef]
6. Fyfe, J. C., Al-Tamimi, R. A., Castellani, R. J., Rosenstein, D., Goldowitz, D. and Henthorn, P. S. 2010. Inherited neuroaxonal dystrophy in dogs causing lethal, fetal-onset motor system dysfunction and cerebellar hypoplasia. *J. Comp. Neurol.* **518**: 3771–3784. [Medline] [CrossRef]
7. Gregory, A., Polster, B. J. and Hayflick, S. J. 2009. Clinical and genetic delineation of neurodegeneration with brain iron accumulation. *J. Med. Genet.* **46**: 73–80. [Medline] [CrossRef]
8. Gregory, A., Westaway, S. K., Holm, I. E., Kotzbauer, P. T., Hogarth, P., Sonek, S., Coryell, J. C., Nguyen, T. M., Nardocci, N., Zorzi, G., Rodriguez, D., Desguerre, I., Bertini, E., Simonati, A., Levinson, B., Dias, C., Barbot, C., Carrilho, I., Santos, M., Malik, I., Gitschier, J. and Hayflick, S. J. 2008. Neurodegeneration associated with genetic defects in phospholipase A(2). *Neurology* **71**: 1402–1409. [Medline] [CrossRef]
9. Hahn, K., Rohdin, C., Jagannathan, V., Wohlsein, P., Baumgärtner, W., Seehusen, F., Spitzbarth, I., Grandon, R., Drögemüller, C. and Jäderlund, K. H. 2015. TECPR2 associated neuroaxonal dystrophy in Spanish water dogs. *PLOS ONE* **10**: e0141824. [Medline] [CrossRef]
10. Kurian, M. A., Morgan, N. V., MacPherson, L., Foster, K., Peake, D., Gupta, R., Philip, S. G., Hendriksz, C., Morton, J. E., Kingston, H. M., Rosser, E. M., Wassmer, E., Gissen, P. and Maher, E. R. 2008. Phenotypic spectrum of neurodegeneration associated with mutations in the PLA2G6 gene (PLAN). *Neurology* **70**: 1623–1629. [Medline] [CrossRef]
11. Malik, I., Turk, J., Mancuso, D. J., Montier, L., Wohltmann, M., Wozniak, D. F., Schmidt, R. E., Gross, R. W. and Kotzbauer, P. T. 2008. Disrupted membrane homeostasis and accumulation of ubiquitinated proteins in a mouse model of infantile neuroaxonal dystrophy caused by PLA2G6 mutations. *Am. J. Pathol.* **172**: 406–416. [Medline] [CrossRef]
12. Morgan, N. V., Westaway, S. K., Morton, J. E. V., Gregory, A., Gissen, P., Sonek, S., Cangul, H., Coryell, J., Canham, N., Nardocci, N., Zorzi, G., Pasha, S., Rodriguez, D., Desguerre, I., Mubaidin, A., Bertini, E., Trembath, R. C., Simonati, A., Schanen, C., Johnson, C. A., Levinson, B., Woods, C. G., Wilmot, B., Kramer, P., Gitschier, J., Maher, E. R. and Hayflick, S. J. 2006. PLA2G6, encoding a phospholipase A2, is mutated in neurodegenerative disorders with high brain iron. *Nat. Genet.* **38**: 752–754. [Medline] [CrossRef]
13. Nibe, K., Nakayama, H. and Uchida, K. 2009. Immunohistochemical features of dystrophic axons in Papillon dogs with neuroaxonal dystrophy. *Vet. Pathol.* **46**: 474–483. [Medline] [CrossRef]
14. Nibe, K., Kita, C., Morozumi, M., Awamura, Y., Tamura, S., Okuno, S., Kobayashi, T. and Uchida, K. 2007. Clinicopathological features of canine neuroaxonal dystrophy and cerebellar cortical abiotrophy in Papillon and Papillon-related dogs. *J. Vet. Med. Sci.* **69**: 1047–1052. [Medline] [CrossRef]
15. Pintus, D., Cancedda, M. G., Macciocu, S., Contu, C. and Ligios, C. 2016. Pathological findings in a Dachshund-cross dog with neuroaxonal dystrophy. *Acta Vet. Scand.* **58**: 37. [Medline] [CrossRef]
16. Schneider, S. A. 2016. Neurodegenerations with Brain Iron Accumulation. *Parkinsonism Relat. Disord.* **22** Suppl 1: S21–S25. [Medline] [CrossRef]
17. Shinzawa, K., Sumi, H., Ikawa, M., Matsuoka, Y., Okabe, M., Sakoda, S. and Tsujimoto, Y. 2008. Neuroaxonal dystrophy caused by group VIA phospholipase A2 deficiency in mice: a model of human neurodegenerative disease. *J. Neurosci.* **28**: 2212–2220. [Medline] [CrossRef]
18. Sisó, S., Ferrer, I. and Pumarola, M. 2001. Juvenile neuroaxonal dystrophy in a Rottweiler: accumulation of synaptic proteins in dystrophic axons. *Acta Neuropathol.* **102**: 501–504. [Medline]
19. Sumi-Akamaru, H., Beck, G., Kato, S. and Mochizuki, H. 2015. Neuroaxonal dystrophy in PLA2G6 knockout mice. *Neuropathology* **35**: 289–302. [Medline] [CrossRef]
20. Tsuboi, M., Watanabe, M., Nibe, K., Yoshimi, N., Kato, A., Sakaguchi, M., Yamato, O., Tanaka, M., Kuwamura, M., Kushida, K., Ishikura, T., Harada, T., Chambers, J. K., Sugano, S., Uchida, K. and Nakayama, H. 2017. Identification of the PLA2G6 c.1579G>A Missense Mutation in Papillon Dog Neuroaxonal Dystrophy Using Whole Exome Sequencing Analysis. *PLoS One* **12**: e0169002. [Medline] [CrossRef]
21. Vandevelde, M., Higgins, R. J. and Oevermann, A. 2012. Degenerative diseases. pp. 166–167, 171. *In*: Veterinary Neuropathology: Essentials of Theory and Practice (Vandevelde, M., Higgins, R. J. and Oevermann, A. eds.), Wiley-Blackwell, Oxford.
22. Wada, H., Kojo, S. and Seino, K. 2013. Mouse models of human INAD by Pla2g6 deficiency. *Histol. Histopathol.* **28**: 965–969. [Medline]
23. Wada, H., Yasuda, T., Miura, I., Watabe, K., Sawa, C., Kamijuku, H., Kojo, S., Taniguchi, M., Nishino, I., Wakana, S., Yoshida, H. and Seino, K. 2009. Establishment of an improved mouse model for infantile neuroaxonal dystrophy that shows early disease onset and bears a point mutation in Pla2g6. *Am. J. Pathol.* **175**: 2257–2263. [Medline] [CrossRef]
24. Yagishita, S. and Kimura, S. 1974. Infantile neuroaxonal dystrophy. Histological and electron microscopical study of two cases. *Acta Neuropathol.* **29**: 115–126. [Medline] [CrossRef]